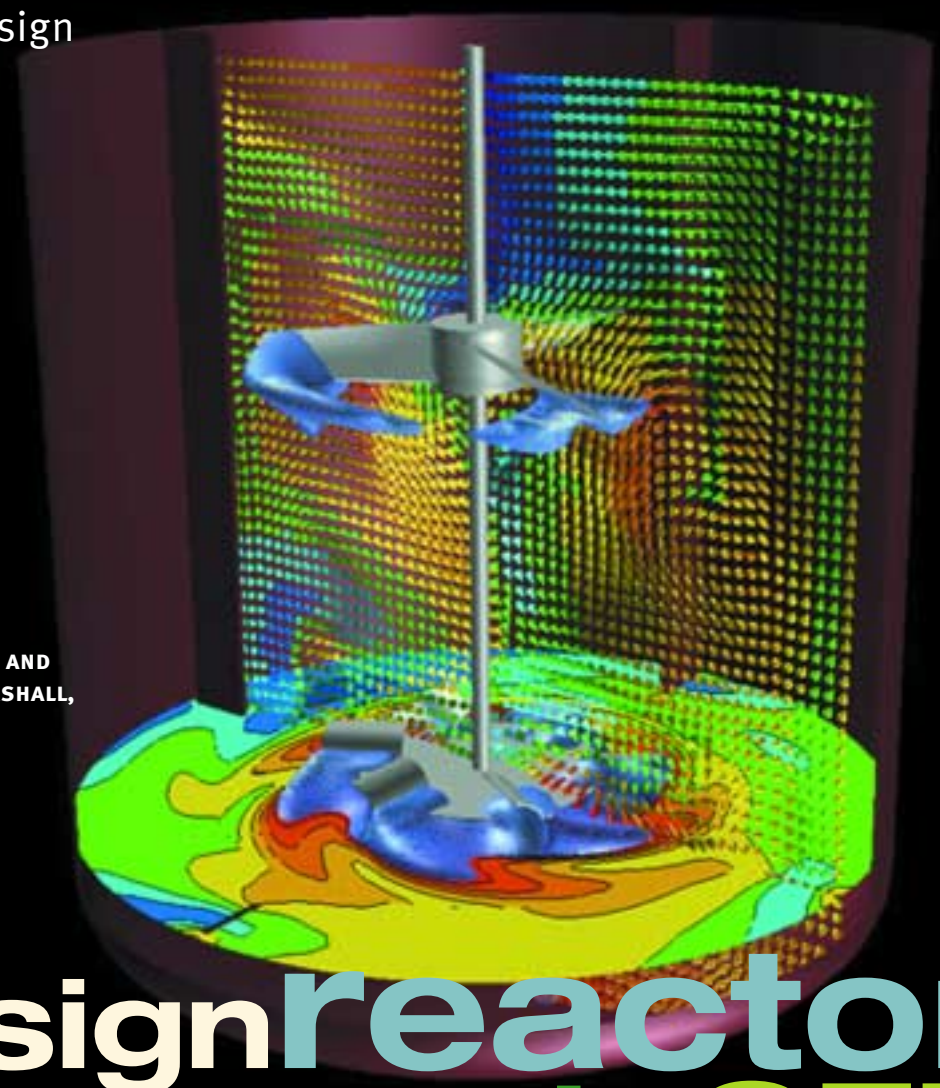

André Bakker,
Ahmad H. Haidari and
Elizabeth M. Marshall,
Fluent Inc.

design reactors via CFD

Using computational fluid dynamics to design commercial-size batch and continuous reactors can eliminate subjective experience and empiricism, and lead to better-designed, more-efficient units.

In addition to their work in the chemical and oil industries, chemical engineers (ChEs) are employed in a wide variety of other industries, such as the production of plastics and synthetic resins, man-made fibers, polymers, paints and varnishes, drugs and pharmaceuticals, agricultural chemicals, fats and oils, foods and beverages, and many others. ChEs are responsible for the design, operation, optimization and troubleshooting of manufacturing operations, and can be involved in applications that range from combustion to biological reactions. All of these industrial applications have one thing in common — raw materials are converted into final products by means of a chemical reaction in an environment that involves fluid flow. Depending upon the physical state of the materials being converted and the operating conditions, different types and scales of reactors are used. These include, but are not limited to, batch; continuous stirred-tank reactors (CSTRs); plug-flow, fluidized, fixed or moving-bed reactors; bubble columns or airlifts; and film reactors. In this article, some of today's most popular methods for simulating reactive flow are reviewed. Examples will emphasize the variety of applications and methods for tackling this complex behavior.

To successfully implement a chemical reaction

developed in the laboratory on an industrial scale, many hurdles are usually encountered. Often, these are related to difficulties in maintaining the same temperatures, pressures, and level of homogeneity of the reactants on a large scale. Furthermore, while the reaction time-constants stay the same on scaleup, other time constants change. Usually, there are significant differences between the residence, feed and mixing times in the laboratory and those on the production floor. In addition to scaleup issues, there is a strong interaction between the molecular reaction process itself, and the thermodynamic, hydrodynamic and mass-transfer processes in the reactor. A detailed understanding of all of these phenomena helps the engineer to design a productive and efficient operation.

This article continues where a prior one on computational fluid dynamics (CFD) modeling ended *(1)*. The basics of CFD will not be reiterated here. We will discuss how to model chemical reactions and the effects of fluid flow on the reaction process. Examples will include Fischer-Tropsch synthesis in a bubble column, polymerization in an autoclave reactor, and ozone decomposition in a fluidized bed.

Chemical reaction overview

Chemically reacting flows are those in which the chemical composition, properties and temperatures change as the result of a simple or complex chain of reactions in the fluid. The reactor is typically simulated using a chemical-reaction model coupled with one of the following four fluid-modeling approaches:

1. A perfectly mixed stirred tank (either batch, semi-batch or continuous)

2. A plug-flow reactor

3. A network of a relatively small number of perfectly mixed and plug-flow reactors

4. A full CFD model.

The calculation time is relatively short for the first three methods. However, such models may not correctly predict the effects of the reactor hydrodynamics on its performance. For example, in a large-scale reactor, the reaction process may be slowed down by local starvation of one of the reactants, poorly mixed reactants, nonuniform catalyst distributions or settled catalysts, thermal nonuniformities or ignition delays.

Thermal nonuniformities may also accelerate reaction processes, and, in some cases, local hot spots may result in product decomposition, or even in thermal runaways or explosions. These phenomena cannot be captured when modeling the reactor using simplified hydrodynamics assumptions (such as perfect mixing), but can be depicted with reasonable accuracy using full CFD models. These have been successfully used for homogenous reaction systems (same state), and heterogeneous reactions (different phases).

When modeling chemical reactors using CFD, the fluid-flow pattern and temperature field are calculated from conservation equations for mass, momentum and enthalpy. These equations can be found in textbooks and will not be reiterated here. For reacting flows, the mixing and transport of chemical species must also be calculated using species-transport equations. Each equation is a statement of conservation of a single species. Multiple-species equations can be used to represent components in a mixture, each of which has different physical properties. To balance the mass transfer from one species to another, reaction rates are used in each species-conservation equation, and have as factors, the molecular weights, concentrations and stoichiometries for that species in all reactions. For the species i', the conservation equation is for the mass fraction of that species, $m_{i'}$, and has the following form:

$$\frac{\partial(\rho m_{i'})}{\partial t} + \frac{\partial(\rho u_i m_{i'})}{\partial x_i} = -\frac{\partial J_{i',i}}{\partial x_i} + R_{i'} + S_{i'} \qquad (1)$$

In this equation i represents one of the three coordinate directions and $J_{i',i}$ is the i^{th} component of the diffusion flux of species i' in the mixture. For laminar flows, $J_{i',i}$ is related to the diffusion coefficient for the species and the local concentration gradients. For turbulent flows, $J_{i',i}$ also includes a turbulent diffusion term, which is a function of the turbulent Schmidt number. $R_{i'}$ is the rate at which the species is either consumed or produced in one or more reactions, and $S_{i'}$ is a general source term for the i^{th} species. Note that i is a coordinate index, while i' is a species index. The general source term can be used for nonreacting sources, such as the evaporated vapor from a heated droplet, for example.

When two or more species are present, the sum of the mass fractions in each cell must add to one. For this reason, if there are n species in a simulation, only $n - 1$ species equations need to be solved. The mass fraction of the n^{th} species can be computed from the required condition:

$$\sum_{i'}^{n} m_{i'} = 1 \qquad (2)$$

For a single-step, first-order reaction, say, A + B $\rightarrow$ R, the reaction rate is given by:

$$R \propto \left(C_A C_B + \overline{c_A c_B}\right) \qquad (3)$$

C_A and C_B denote the mean molar concentrations of reactants A and B, while c_A and c_B denote the local concentration fluctuations that result from turbulence. When the species are perfectly mixed, the second term on the right-hand side approaches zero. If the species are not perfectly mixed, this term will be negative and will re-

Nomenclature

a = interfacial area per volume, m^{-1}
A, B = Magnussen mixing rate constants
A_k = Arrhenius constant for reaction k
$C_{j'}$ = concentration of species j', mol/m^3
E_k = activation energy for reaction k, J/mol
$J_{i',i}$ = diffusion flux of species i' in direction I, kg/m^2•s
k = turbulent kinetic energy, m^2/s^2
k_i = mass-transfer rate, mol/m^3•s
k_l = liquid-side mass-transfer coefficient, m/s
$K_{i',k}$ = reaction rate of species i' in reaction k
$m_{i'}$ = mass fraction of species i'
$M_{i'}$ = molecular weight of species i'
R = universal gas constant, J/mol•K
$R_{i'}$ = generalized source term for reactions in the species i' transport equation, kg/m^3•s
$R_{K_i',k}$ = kinetic reaction rate for species i' in reaction k, kg/m^3•s
$R_{M1\text{-}i',k}$ = mixing-limited reaction rate for the reactant species i' in reaction k, kg/m^3•s
$R_{M2\text{-}i',k}$ = mixing-limited reaction rate for the product species i' in reaction k, kg/m^3•s
S = strain rate, s^{-1}
$S_{i'}$ = Net species source term in the species i' transport equation
t = time, s
T = temperature, K
U_i = velocity in the direction i, m/s
x_i = spatial coordinate in direction i, m

Greek letters

β_k = temperature exponent in Arrhenius rate expression
ε = turbulent kinetic energy dissipation rate, m^2/s^3
$\eta_{j',k}$ = exponent for concentration of species j' in reaction k
$\nu_{i'}$ = stoichiometry of species i'
ρ = liquid density, kg/m^3

duce the reaction rate. The estimation of this correlation term is not straightforward and numerous models are available for this purpose. Its presence shows, however, that the reaction rate should incorporate not only the mean concentrations of the reactant species, but also include the turbulent fluctuations of the reactant species as well, since the latter give an indication of the degree to which these species are mixed.

One popular method for computing the reaction rates as a function of both mean concentrations and turbulence levels is through the Magnussen model *(2)*. Originally developed for combustion, it can also be used for liquid reactions by tuning some of its parameters. The model consists of rates calculated by two primary means. An Arrhenius, or kinetic rate, $R_{K_i',k}$, for species i' in reaction k, is governed by the local mean species concentrations and temperature in the following way:

$$R_{K_i',k} = -\nu_{i',k} M_i A_k T^{\beta_k} \exp\left(-\frac{E_k}{RT}\right) \prod_{j'=1}^{N} \left[C_{j'}\right]^{\eta_{j',k}} =$$

$$K_{i',k} M_{i'} \prod_{j'=1}^{N} \left[C_{j'}\right]^{\eta_{j',k}} \qquad (4)$$

This expression describes the rate at which species i' is consumed in reaction k. The constants A_k and E_k, the Arrhenius pre-exponential factor and activation energy, respectively, are adjusted for specific reactions, often as the result of experimental measurements. The stoichiometry for species i' in reaction k is represented by the factor $\nu_{i',k}$, and is positive or negative, depending upon whether the species serves as a product or reactant. The molecular weight of the species i' appears as the factor $M_{i'}$. The temperature, T, appears in the exponential term and also as a factor in the rate expression, with an optional exponent, β_k. Concentrations of other species, j', involved in the reaction, $[C_{j'}]$, appear as factors with optional exponents associated with each. Other factors and terms not appearing in Eq. 4, can be added to include effects such as the presence of nonreacting species in the rate equation. Such so-called third-body reactions are typical of the effect of a catalyst on a reaction, for example. Many of the factors appearing in Eq. 4 are often collected into a single rate constant, $K_{i',k}$.

In addition to the Arrhenius rate, two mixing rates are computed that depend upon the local turbulent kinetic energy and dissipation rate. One rate, $R_{M1_i',k}$, involves the mass fraction of the reactant in reaction k, m_R, that returns the smallest rate:

$$R_{M1_i',k} = \nu_{i',k} M_{i'} A \rho \frac{\varepsilon}{k} \frac{m_R}{\nu_{R,k} M_R} \qquad (5)$$

where the subscript R refers only to the reactant species, $i' = R$. The other mixing rate, $R_{M2_i',k}$, involves the sum over product-species mass-fractions, m_P:

$$R_{M2_i',k} = \nu_{i',k} M_{i'} AB \rho \frac{\varepsilon}{k} \frac{\sum_P m_P}{\sum_j^N \nu'_{j',k} M_j} \qquad (6)$$

For gaseous-combustion models, constants A and B often have values of 4.0 and 0.5, respectively. These values can be adjusted for different types of reactions, such as those involving liquids *(3)*.

After the rates in Eqs. 4, 5 and 6 are computed, the smallest or slowest, is used as a source term in the species-transport equations for all species involved in any given reaction. The basic idea behind the Magnussen model is that, in regions with high-turbulence levels, the eddy lifetime, k/ε, is short, mixing is fast, and, as a result, the reaction rate is not limited by small-scale mixing. In this limit, the kinetic rate usually has the smallest value. On the other hand, in regions with low turbulence levels, small-scale mixing may be slow and limit the reaction rate. In this limit, the mixing rates are more important.

This common model has been most extensively used with turbulence models such as the k-ε style and Reynolds stress models. However, there is a trend to-

wards combining chemically reacting flow modeling with large-eddy-simulation (LES) and even direct-numerical-simulation (DNS) turbulence modeling methods. These models do not explicitly calculate the eddy dissipation rate ε, and so it is necessary to replace ε in the above rate equations with a suitable substitute. This is typically done by replacing the term ε/*k*, which is the reciprocal of the eddy lifetime, with the magnitude of the local strain rate $\bar{S}$:

$$\bar{S} = \sqrt{2S_{ij}S_{ij}} \qquad S_{ij} = \frac{1}{2}\left(\frac{\partial u_j}{\partial x_i} + \frac{\partial u_i}{\partial x_j}\right) \tag{7}$$

The Magnussen model was initially developed for simple, one- or two-step reaction sets, in which all reaction rates are fast relative to the small-scale mixing. However, this model has even found use for more complex systems. Recently, for such a system, an extension of the Magnussen has been developed *(4)*, termed the eddy-dissipation-concept (EDC) model. This model assumes that the reaction occurs in small, turbulent structures, called fine-scales. A volume fraction of the fine-scales is calculated, which depends on the kinematic viscosity of the fluid, the energy-eddy-dissipation rate, and the turbulent kinetic energy. Reactions are then assumed to occur in the fine, turbulent structures, over a time-scale that depends upon the kinematic viscosity and the energy-dissipation rate. A source term for each chemical species is then calculated that depends upon the volume fraction of the fine-scales, the time-scale, and the difference in species concentrations between the fine-scale structures and the surrounding fluid. This extension of the Magnussen model provides improved accuracy for complex, multistep reaction sets in which not all reactions are fast relative to the rate at which small-scale mixing occurs.

Numerous other reaction models exist that can be coupled to the CFD calculation. For example, a collection of reacting species can be described by a mixture fraction, which, under certain circumstances, is a conserved quantity. This so-called PDF modeling approach takes its name from the probability-density-function method used to describe the turbulence/chemistry interaction in the model. It is based on the assumptions of infinitely fast reactions and chemical equilibrium at all times. Rather than solve conservation equations for multiple species, these equations are solved for the mean and variance of the mixture fraction. The variance in the fraction is representative of fluctuations in the species concentrations. Thus, while the kinetic-rate expression uses time-averaged values for species mass fractions, the PDF model allows for fluctuations in these quantities. Auxiliary reaction calculations allow for the extraction of intermediate and product species as a function of the mixture fraction and temperature distributions in the final CFD solution. While this model has many benefits for gaseous combustion systems, it is not the best choice for liquid reactions that are typical of most chemical process industries (CPI) applications, where reaction rates can fall anywhere from very fast to very slow when compared with typical mixing rates.

Another reaction modeling approach incorporates the methodology used to describe micromixing, or mixing on the smallest scales *(5, 6)*. In the context of a CFD calculation, micromixing is on a scale that is smaller than a typical computational cell. Macromixing, on the other hand, is responsible for large-scale blending, and mesomixing is in between. The identification of these mixing regimes is drawn from assumptions at the core of turbulence modeling theory, namely that turbulence energy is generated in large eddies within a domain, and it cascades to successively smaller eddies before being dissipated on the smallest scales. This cascade of turbulence is associated with a cascade of mixing, from macromixing on the large scales, to mesomixing throughout the mid-scales, to micromixing on the sub-grid scales.

One motivation for the interest in micromixing in liquid reactions is that micromixing must occur before reactions can take place. It therefore plays an important role when the reaction times are on the same order as the mixing times. Micromixing models typically use a mixture-fraction approach, employing a PDF formulation for the turbulence-chemistry interaction. The micromixing models are incorporated through calculating the variance of the mixture fraction.

Fischer-Tropsch synthesis in a bubble column

Bubble columns are used in the CPI for many applications, one of which is Fischer-Tropsch synthesis. In this process, steam/oxygen gasification of coal or other hydrocarbons produces a mixture of hydrogen and carbon monoxide. These gases react in a column of water to form a variety of hydrocarbons in the liquid state. The products are collectively referred to as synthesis liquids and the gas-to-liquid conversion process is called syngas conversion. Both hydrodynamics and chemical reactions are important in determining the amount of syngas conversion that takes place in any given system. To simulate the hydrodynamics of the liquid/gas system, the Eulerian multiphase model is used. As described in Ref. 1, this model uses separate sets of fluid equations for each phase, in this case the gas and liquid, and couples them through pressure, mass, momentum and heat exchange. To simulate the chemical reaction between the phases, chemical species are defined in each phase. The reactions give rise to interphase mass transfer and the results are used to predict syngas conversion in an industrial-sized bubble column — the reactor.

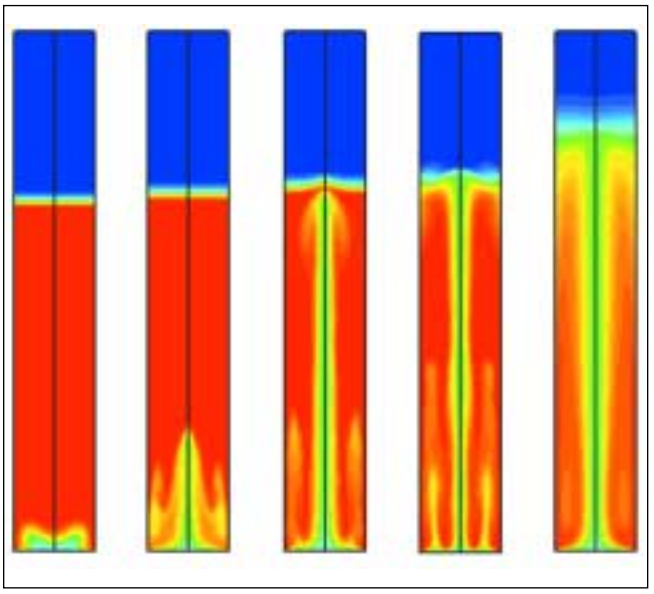

Figure 1. Liquid-phase volume-fraction at 5, 10, 15, 20 and 60 s.

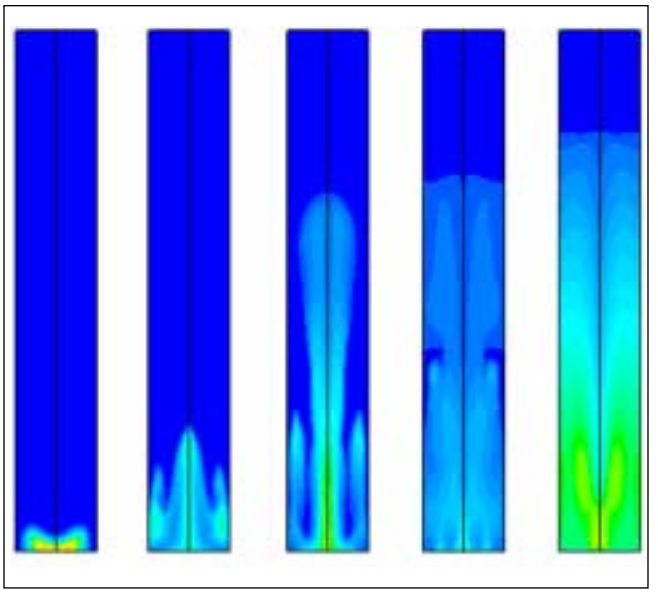

Figure 2. Liquid-product concentration at 5, 10, 15, 20 and 60 s.

As an example, consider the reaction between two gas-phase reactants, CO (g) and H_2 (g), in a column of water *(7)*. The gases enter the column through an inlet on the bottom. The products are in the liquid phase, and are water, H_2O (l), and a collection of hydrocarbons in the methylene group, $–(CH_2)$ (l):

$$CO\ (g) + H_2\ (g) \rightarrow\ –(CH_2)\ (l) + H_2O\ (l) \qquad (8)$$

The reaction rate is assumed to be dominated by mass transfer across the gas/liquid interface:

$$k_{i'} = k_l\, a(\,[C_{eq,\,i'}] - [C_{i'}]) \qquad (9)$$

where i' represents the reactants, either CO or H_2. The quantity k_l is the liquid-side mass-transfer coefficient and a is the gas/liquid interfacial area. $[C_{eq,\,i'}]$ is the equilibrium concentration of the gas species, i', in the liquid phase and can be estimated by the partial pressure of the species. $[C_{i'}]$ is the local concentration of the reactant gas species i'. Values for $k_{i'}$ are computed for each of the gas-phase species, and the smallest (or slowest) one is used in the calculation. Additional reaction steps produce C_nH_{2n}, C_nH_{2n+2}, $C_nH_{2n+1}OH$ and CO_2. These are not modeled here.

A two-dimensional (2-D) axisymmetric model of the an industrial-sized bubble column is used. The column is 7 m in dia. and the initial liquid level is 30 m in height. Two gas-phase species are used in the model, as are two-liquid phase species. The column is initially filled with pure water, and the gas space on top is initially filled with pure hydrogen. A gas inlet at the bottom of the column injects a mixture of CO (87.5%) and H_2 (12.5%) at a speed of 0.15 m/s. The chemical reactions are accounted for as balanced- species sources in each phase. The model also computes the mass-transfer rate across the gas/liquid interface.

Figure 1 shows the volume fraction of liquid after 5, 10, 15, 20 and 60 s of operation. Red corresponds to pure liquid, and blue, to pure gas. As time progresses, gas fills the liquid, and causes the liquid level to rise. The makeup of the liquid begins as pure water, but changes over time to include hydrocarbon products, as well. The gas is injected through a circular opening with a diameter slightly less than the column diameter. The inlet velocity profile is constant, but already starts to deform in the liquid after 5 s, as is evident in the leftmost graphic in Figure 1.

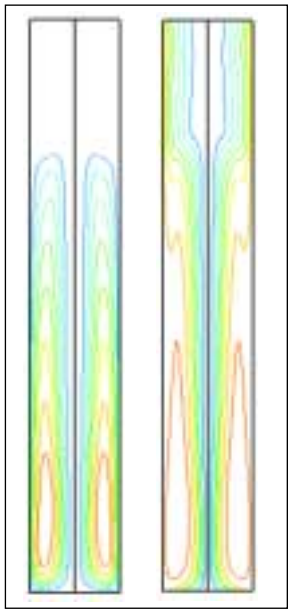

Figure 3. Stream-function contours lines at 60 s for the liquid (left) and gas (right) phases.

Figure 2 shows the mass fraction of the methylene-group hydrocarbons (one of the products in the liquid phase) at 5, 10, 15, 20 and 60 s. The increased amount of product near the bottom of the column is the result of recirculation currents that become established during

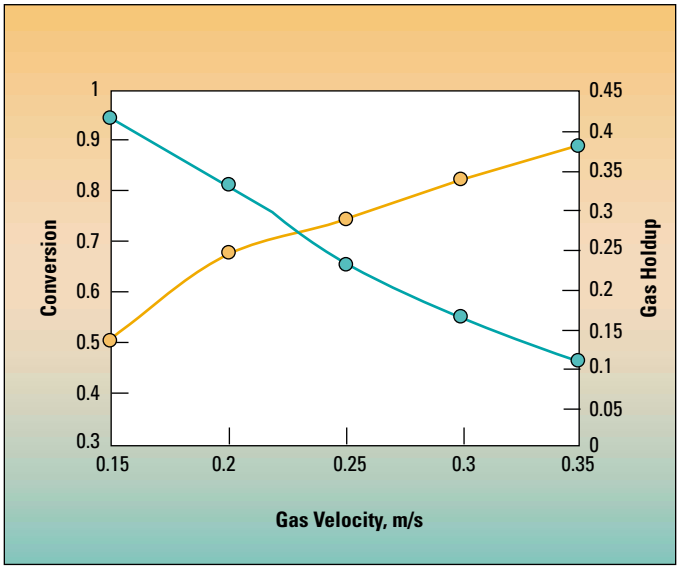

Figure 4. The conversion rate (green) and gas holdup (orange) as functions of the gas velocity.

operation. These currents are radially outside the rising gas stream at the center of the column, which can be seen forming in Figure 1.

In Figure 3, stream-function contour-lines for the liquid (left) and gas (right) phases are shown after 60 s. At this point, the system has reached steady operation, even though fluctuations in the flow patterns continue. The liquid phase is characterized by a strong recirculation current. The gas phase, on the other hand, has some recirculation, and some short-circuiting of gas from the inlet to the outlet at the top of the column. It is the recirculation of gas and liquid in the vessel that continues to feed the reaction and produce the highest concentration of product near the bottom of the column, as was shown in Figure 2.

Figure 4 shows the gas holdup and the syngas conversion as functions of the gas velocity. For low gas rates, the gas momentum is low, so the gas cannot lift the liquid high enough to hold a significant quantity of gas. Thus, the gas holdup at low gas rates is low. At high gas rates, there is more momentum in the gas phase to push the liquid up, so that it can hold more gas. The gas holdup in this regime is high. This expected hydrodynamic result is predicted by the CFD calculation.

At low gas rates, the residence time in the unit is high, so conversion of the gas-to-liquid is high. For high gas rates, the opposite is true. The residence time for the gas is lower, and the subsequent conversion is reduced. This result is also shown in Figure 4. The results in Figures 1 and 2 correspond to the lowest flowrate shown, 0.15 m/s.

This example shows how a reacting multiphase flow can be modeled. The problem definition is further complicated by the fact that the reactants are in one phase, while the products are in the other. The results illustrate that complex simulations of this type can be carried out successfully using CFD.

Polymerization in an autoclave reactor

Low-density polyethylene (LDPE) reactors are used to manufacture polymer products. The reactors are typically of the tubular or autoclave variety. To make the polymer, a minute amount of initiator is added to a (single-molecule) monomer. Several reaction steps take place in which the monomer is transformed to a polymer with a range of chain lengths (corresponding to a range of molecular weights). Heat is released in many of the reactions, and one goal of LDPE reactor design is to prevent hot spots that give rise to thermal runaways, which are characterized by an undesired product distribution.

In this example *(7)*, the nearly infinite set of reactions in the chain is approximated by the following six finite-rate reactions using the method of moments *(8)*.

Reaction 1: Initiator decomposition: $I \rightarrow 2A$
Reaction 2: Chain initiation: $A + M \rightarrow R_1$
Reaction 3: Chain propagation: $M + R_x \rightarrow R_{x+1}$
Reaction 4: Chain transfer to monomer: $M + R_x \rightarrow P_x + R_1$
Reaction 5: Disproportionation termination: $R_x + R_y \rightarrow P_x + P_y$
Reaction 6: Combination termination: $R_x + R_y \rightarrow P_{x+y}$

where I is the initiator, A the initiator radical, M the monomer, R_x is a radical of arbitrary length, R is the total radical, ΣR_x, and P is the total polymer, ΣP_x. As a consequence of the method of moments, quantities that describe the product distribution can also be computed. These include the molecular-weight distribution, which, if narrow, indicates a high-quality (uniform) product. Other predicted quantities include initiator consumption rate, monomer conversion, total radical and total polymer concentration gradients, and the temperature profile.

A 3-D model of an autoclave reactor

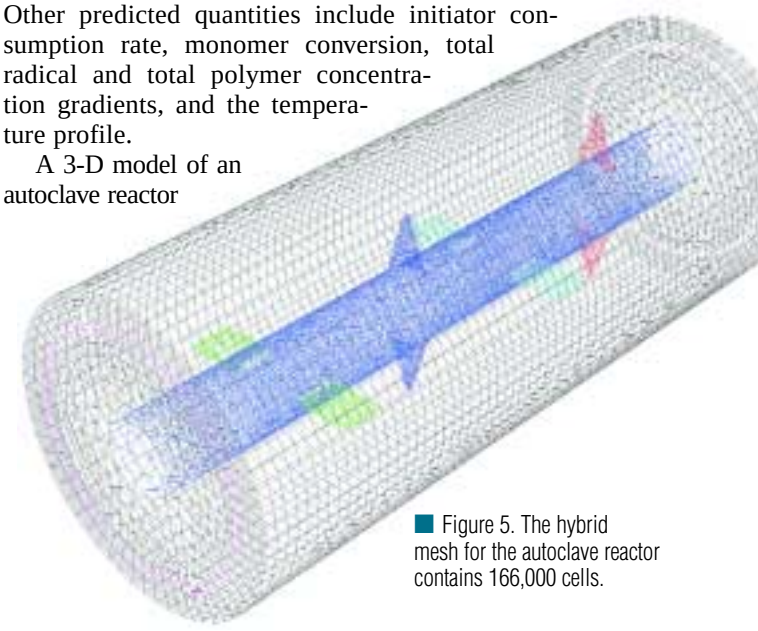

Figure 5. The hybrid mesh for the autoclave reactor contains 166,000 cells.

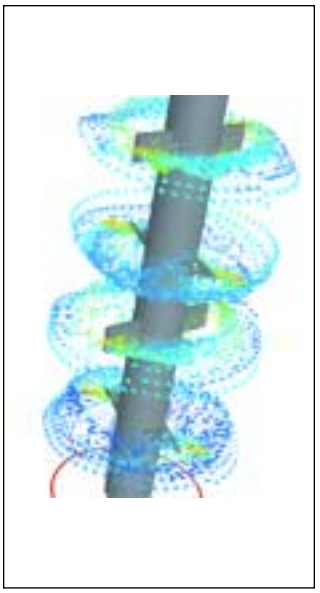

Figure 6. The velocity field is highly swirling.

Figure 7. Temperature increases from 460 K to 540 K in the reactor.

Figure 8. Contours of the molecular-weight distribution are used to assess the range of molecular weights in the product.

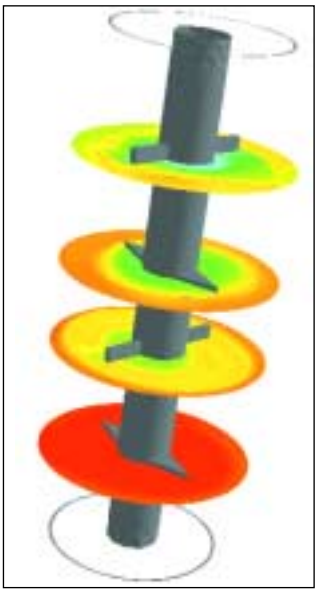

Figure 9. Viscosity is shown to increase as the makeup of the polymer mixture changes within the reactor.

is described here. It incorporates the method of moments for the reaction with a CFD calculation for the flow field. The monomer used is ethylene. The viscosity of the mixture is computed as a function of the temperature and concentrations of these species and those of the intermediate polymers (or radicals) and product polymers.

Figure 5 shows the hybrid mesh of 166,000 cells used for the simulation. The reactor contains both paddle and twisted-blade impellers, which are modeled using a sliding mesh, a technique that is common for accurate simulation of rotating equipment. The initiator is premixed with the monomer and injected into the reactor through an annular ring. The RNG k-ε model is used to account for the turbulence in the highly swirling flow.

The velocity vectors in Figure 6 show the high swirl induced by the rapidly rotating (250 rpm) impellers in the unbaffled vessel. Four axial slices are used in the next three figures (Figures 7–9) to show the progression of different problem variables as the mixture advances through the reactor. In these figures, the inlet annulus is at the top of the figure and the outflow annulus is at the bottom. (Both are shown as grey circles.)

In Figure 7, the temperature contours increase from the inlet temperature of 460 K to a high of 544 K near the exit. The thermal decomposition of the ethylene monomer could occur at 544 K, giving rise to a poor product distribution. This high temperature is partly the result of an adiabatic thermal boundary condition on the reactor walls that was used in the simulation. The contours of the molecular weight distribution in Figure 8 vary from 41,500 to 41,900, or by about 1%. The narrower this distribution, the higher the quality of the product. The molecular viscosity is computed by a custom function that incorporates the concentrations of the various species in the vessel, as well as the temperature. Its value increases from a low of about 0.019 kg/m•s to a high of about 0.026 kg/m•s, as the chains of radicals and polymer product increase in length in the reactor, as shown in Figure 9.

The results of this simulation are in reasonably good agreement with Ref. 9. They provide information about important reactor characteristics, including the temperature and viscosity distribution, as well as the spread of molecular weights in the resulting product. Comprehensive results such as these can be used to troubleshoot (and help redesign) problem installations in which the product quality is not optimal.

Ozone conversion in a fluidized-bed reactor

The conversion of ozone gas to oxygen gas is another example of a reactions in a multiphase system *(10)*. The decomposition process occurs in a fluidized bed, where the particles in the bed serve as a catalyst. "Bed conversion" refers to the process by which the passage of one material through the bed is converted to another during transit. Design of the system for optimum conversion strongly depends upon knowledge of both hydrodynamics and chemical reactions. It is essential, therefore, to model both phenomena together in a CFD simulation. An Eulerian-granular multiphase flow model is used,

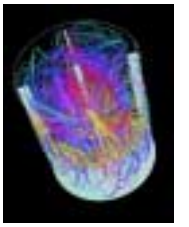

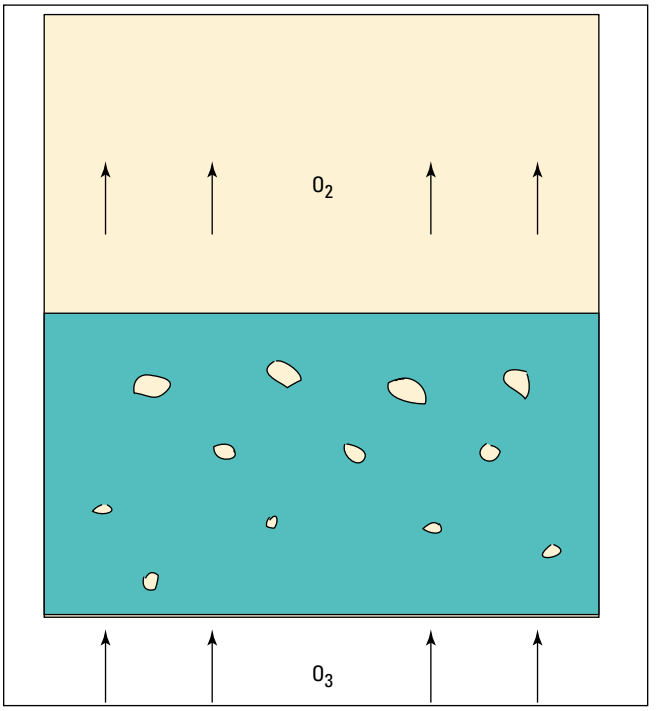

Figure 10. A schematic of the ozone decomposition system.

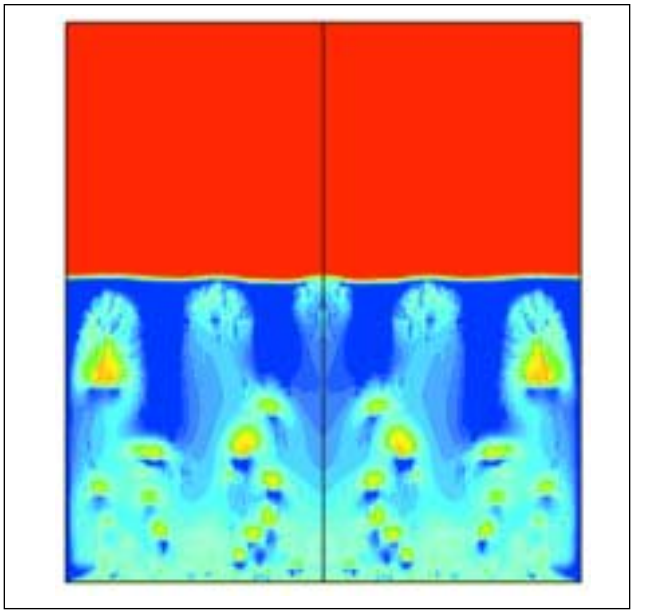

Figure 11. The fluidized bed after 0.5 s of operation.

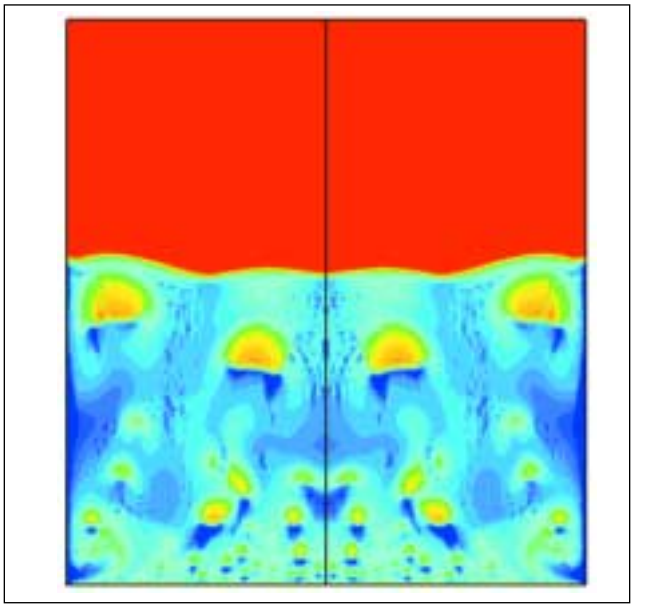

Figure 12: The fluidized bed after 1.0 s of operation.

which has a special treatment for the granular phase that constitutes the bed. It is combined with a multispecies, reacting gas phase model to predict ozone decomposition (and conversion to oxygen) in the fluidized bed.

A 2-D axisymmetric problem is a useful means of studying this process. A column 0.229 m in dia. and 0.25 m high is used, modeled with a grid of 110 × 70 cells. At rest, the bed is 0.115 m high. It contains catalyst particles 117 μm in dia. The decomposition of ozone is brought about by sand particles impregnated with iron oxide in the bed. The decomposition reaction is first-order for the two gas species:

$$O_3 \rightarrow 1.5\ O_2 \qquad (10)$$

The decomposition rate is expressed as:

$$K = 1.57\ a\ [O_3] \qquad (11)$$

where a is the volume fraction of the catalyst and $[O_3]$ is the concentration of ozone. The reaction takes place in the bed region only. The calculations are done for superficial velocities in the range from 4 to 14 cm/s.

A schematic of the device is shown in Figure 10. Ozone enters the bed in a uniform flow from the bottom. As it passes through the bed, it interacts with the catalyst and is converted to oxygen. Figure 11 shows the gas volume fraction in the bed at t = 0.5 s. The flow field is the same whether the reaction in the gas phase is taking place or not. The bubbles are formed near the bottom of the bed and migrate upwards. The bubble shape and size are grid-dependent. When a coarse mesh is used, the bubbles are fewer in number and rounder. When a fine mesh is used, the bubbles are denser and more irregular. The number of bubbles has a significant impact on the conversion. The more bubbles in the domain, the higher the conversion.

Figure 12 shows the gas volume fraction at a t = 1 s. Notice how the upper surface of the bed is lifted by the approaching bubbles. While some large bubbles stand out, the bed itself is filled with small bubbles to a greater or lesser degree (as indicated by the shades of blue and

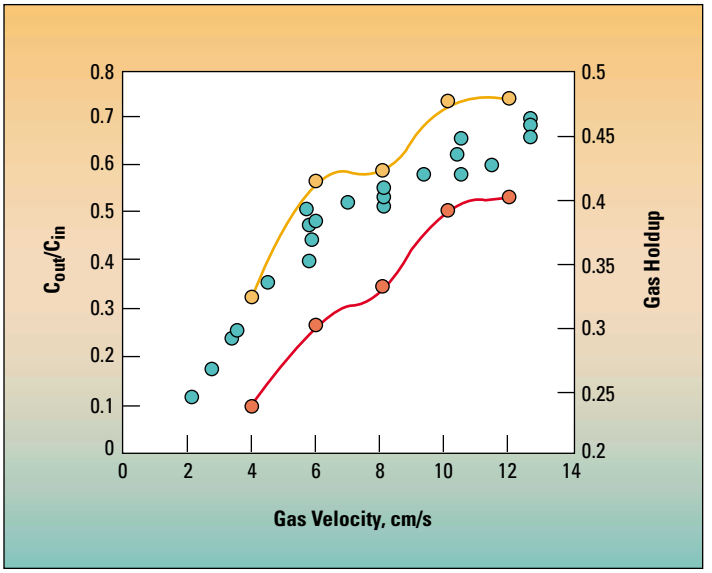

Figure 13. The orange circles show the predictions for the ratio between C_{out}/C_{in} for O_3, which is equal to (1 - conversion). The green circles show the corresponding experimental data (*9*). The red circles are the predictions for the gas holdup. All data are shown as functions of superficial gas velocity.

green). A bed filled with bubbles in this manner is the desired hydrodynamic state for optimum conversion.

Figure 13 shows the conversion curve and gas holdup as functions of the gas velocity at the inlet on the floor of the bed. The gas holdup is defined as the ratio of the gas in the bed to the total volume of the bed. The curve shows that the gas holdup increases with gas velocity up to a point, after which saturation occurs. At low velocities, the increasing gas velocity forces the bed to lift more. At higher velocities, the bed can no longer rise and hold additional gas, and saturation occurs.

The conversion curve is plotted along with data from the literature *(9)*, and good agreement is in evidence. When the quantity C_{out}/C_{in} is small, a small amount of ozone exits at the top of the bed, meaning that conversion to oxygen is high. This occurs at low velocities, where the residence time of ozone in the bed is long. At high velocities, C_{out}/C_{in} is large, meaning that the conversion to oxygen is poor. This is due to the fact that the residence time is shortened, allowing less time for the catalytic reaction to occur. The technique used in this example could be applied to determine optimum flowrates for the incoming ozone flow, or to test modifications of the bed design, such as the aspect ratio or the addition of baffles or other internals. Validation of a laboratory-scale model could also be the basis of scaleup designs for an industrial setting.

Expanding the toolbox

In the CPI, new chemical materials traditionally were developed empirically via trial-and-error processes that took years. Recent advances in the computer modeling of molecular chemistry, however, combined with empirical combinatorial chemistry methods promise to significantly reduce the cycle times related to the discovery of new chemical products.

The requirements to develop and produce new products to create revenue growth, and more stringent efficiency requirements to improve profitability, directly affect the chemical engineer's job. New products may require new and more-difficult-to-operate chemical reaction processes to be productive in mass quantities. Improved efficiency requirements may require fine-tuning of existing processes, or the replacement of tried-and-true methods with completely new ones. An example of the latter would be the replacement of large, batch reactors with smaller continuous units to obtain process intensification.

The classical working methods of chemical engineers, which rely heavily on empiricism, practical experience, extensive consultation of printed handbooks, and manual calculations, may no longer be suited for this new and changing environment. More-advanced design and analysis tools are needed. And indeed, many computer-based design tools have been developed.

Flowsheet-modeling software can analyze the operation of complete plants. To make the models tractable, simplified hydrodynamic models with reduced reaction sets are often used for the individual chemical reactors. On the other end of the spectrum, specialized software exists to model complex chemistry. Such software can handle stiff (*i.e.*, those with a large difference in timescales and are especially difficult) reaction sets with hundreds of surface and volumetric reactions, but the software is neither suitable to model complete plants nor able to take into effect the hydrodynamics of the reactor. In between these two extremes falls CFD software, which can model both chemical reactions and the link with reactor hydrodynamics dynamics. CFD software is generally used to model individual plant components, and not the whole process at once. When tied to flowsheet-modeling software, however, it can provide more accurate flow-field data (averaged velocities or temperatures) about unit operations than the simplified assumptions normally used for input.

Indeed, the current trend is to integrate these various pieces of software. New chemical products are being developed by using a combination of molecular modeling software and combinatorial chemistry. Once the new materials and the operating conditions required for the reaction process have been identified in the laboratory, the production process can be designed by using the flowsheet model as the basis.

The flowsheet model uses its standard models for non-reaction-critical components such as pipelines, pumps and conveyors. For the critical components, an advanced CFD model automatically replaces the one-dimensional models currently included in the flowsheet

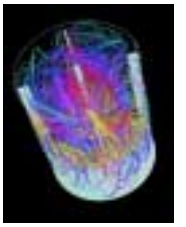

software. The CFD software automatically exchanges the required data with the flowsheet model. It models both the fluid dynamics of the reactor and the chemical reaction process. For complex reaction sets, the CFD software may automatically call a specialized chemical reaction program that replaces its standard chemical reaction solver, and solves the complex reaction set for every cell in the CFD domain at every fluid-flow timestep. Although not yet generally commercially available, such integrated systems have been implemented on a custom basis. It is expected that within a few years, software will be commonly available that includes flowsheet modeling, reactor hydrodynamics modeling, and fully integrated complex reaction models.

As discussed, one of the most challenging tasks for a ChE is the scaleup of a laboratory-scale reactor to a full-size chemical plant. Full-scale experimentation is usually out of the question. However, in the past, scaleup based on a purely theoretical approach was also considered impossible. Current methods therefore rely on a hybrid approach that combines extrapolation of laboratory- and pilot-scale data, dimensional analysis, theoretical analysis, empirical correlations and practical experience.

The rapid increase in computer power, combined with theoretical advances in the fields of chemical reaction and fluid dynamics, are increasing the role of theoretical analysis. This is accelerated by the changes in training ChEs currently receive in college. In the past, ChEs were trained by getting their hands dirty, performing laboratory experiments and interpreting the results using dimensional analysis. Today's engineers are much more familiar with designing equipment on a computer than actually building it by hand. It is therefore to be expected that in the future, the design and scaleup of chemical plants will be done completely based on theoretical and computational analysis, reducing the role of subjective personal experience and empiricism. CEP

Literature Cited

1. **Bakker A., *et al.*,** "Realize Greater Benefits from CFD," *Chem. Eng. Progress*, **97** (3), pp. 45–53 (Mar. 2001).
2. **Magnussen, B. F., and B. H. Hjertager,** "On Mathematical Models of Turbulent Combustion with Special Emphasis on Soot Formation and Combustion," *Proc. 16th Int. Symp. on Combustion*, The Combustion Institute, Pittsburgh, PA (1976).
3. **Bakker, A., and J. B. Fasano,** "Time Dependent, Turbulent Mixing and Chemical Reaction in Stirred Tanks," paper presented at AIChE Annual Meeting, St. Louis, MO (Nov. 1993), also published in "AIChE Symposium Series," No. 299, **90**, "Industrial Mixing Technology: Chemical and Biological Applications," G. B. Tatterson, volume editor, pp. 71–78 (1994).
4. **Gran, I. R., and B. F. Magnussen,** "A Numerical Study of a Bluff-Body Stabilized Diffusion Flame: Part 2; Influence of Combustion Modeling and Finite-Rate Chemistry," *Combustion Sci. and Tech.*, pp. 119–191 (1996).
5. **Fox, R. O.,** "On the Relationship between Lagrangian Micromixing Models and Computational Fluid Dynamics," *Chem. Eng. and Proc.*, **37**, pp. 521–535 (1998).
6. **Hannon, J.,** "Mixing and Chemical Reaction in Tubular Reactors and Stirred Tanks," PhD thesis, Cranfield Inst. of Technology, Cranfield, U.K. (1992).
7. **Zhou, W., *et al.*,** "Application of CFD in Modeling Multiphase Reactors," paper presented at Chemical Reaction Engineering VII: Computational Fluid Dynamics, Quebec City, Canada — sponsored by the United Engineering Foundation, New York — (Aug. 6–11, 2000).
8. **Kiparissides, C., *et al.*,** "Dynamical Simulation of Industrial Poly(vinyl chloride) Batch Suspension Polymerization Reactors," *Ind. Eng. Chem. Res.*, **36** (4), p. 1253 (1997).
9. **Read, N. K., *et al.*,** "Simulations of a LDPE Reactor Using Computational Fluid Dynamics," *Reactors, Kinetics, and Catalysis*, **43** (1), p. 104 (1997).
10. **Fryer, C., and O. E. Potter,** "Experimental Investigation of Models for Fluidized Bed Catalytic Reactors" *AIChE J.*, **22**, pp. 38–47 (1976).

ANDRE BAKKER is the regional consulting manager at Fluent Inc.(10 Cavendish Court, Centerra Resource Park, Lebanon, NH 03766-1442; Phone: (603) 643-2600; Fax: (603) 643-3967; E-mail: ab@fluent.com). Bakker is an internationally recognized expert in industrial mixing and CFD modeling of chemical engineering applications. His specialization includes experimental and computational fluid mixing. He holds engineering and doctorate degrees from Delft Univ. of Technology in the Netherlands, both in applied physics. He has coauthored more than 50 technical articles and presentations on fluid dynamics and mixing. Bakker is a member of AIChE.

AHMAD H. HAIDARI is the chemical team leader at Fluent Inc. (Lebanon, NH; Phone: (603) 643-2600; Fax: (603) 643-3967; E-mail: ah@fluent.com). Haidari has 15 years of experience in the application of flow modeling in addressing industrial-process-equipment design, process troubleshooting, analysis and scaleup. He holds a PhD in mechanical engineering from Lehigh Univ., is a member of AIChE, and has made numerous presentations and written publications on modeling chemical process equipment.

ELIZABETH M. MARSHALL is the technical marketing archive manager at Fluent Inc. (Lebanon, NH; Phone; (603) 643-2600; Fax: (603) 643-3967; E-mail: emm@fluent.com). She has been with Fluent for more than ten years. She has extensive experience in a wide range of industrial applications, with special focus in the chemical process and mixing areas. She holds a bachelor's degree in mathematics from St. Lawrence Univ. and a PhD in physics from Dartmouth College.

Acknowledgment

The authors wish to acknowledge the contributions of the following individuals: Jay Sanyal and Wei Zhou for their contributions to the Fischer-Tropsch model; Bin Yang, Wei Zhou, Madhava Symlal, and Sergio Vasquez for their contributions to the ozone decomposition model; Wei Zhou for her contributions to the LDPE model; and Heshmat Massah, Jeff Ma and Madhusuden Agrawal for many useful discussions and advice.